scientific reports

Check for updates

OPEN

Preparation and properties of silver-carrying nano-titanium dioxide antimicrobial agents and silicone composite

Dongdong Hao[1], Yuxuan Zhang[2]✉, Yonghong Ding[3] & Qiuyu Yan[1]

The characteristics of dopamine self-polymerization were used to cover the nano-titanium dioxide (TiO_2) surface and produce nano-titanium dioxide-polydopamine (TiO_2-PDA). The reducing nature of dopamine was then used to reduce silver nitrate to silver elemental particles on the modified nano-titanium dioxide: The resulting TiO_2-PDA-Ag nanoparticles were used as antimicrobial agents. Finally, the antibacterial agent was mixed with silicone to obtain an antibacterial silicone composite material. The composition and structure of antibacterial agents were analyzed by scanning electron microscopy, transmission electron microscopy, X-ray photoelectron energy spectroscopy, and X-ray diffraction. Microscopy and the antibacterial properties of the silicone antibacterial composites were studied as well. The TiO_2-PDA-Ag antimicrobial agent had good dispersion versus nano-TiO_2. The three were strongly combined with obvious characteristic peaks. The antibacterial agents were evenly dispersed in silicone, and the silicone composite has excellent antibacterial properties. Bacillus subtilis (*B. subtilis*) adhesion was reduced from 246×10^4 cfu/cm^2 to 2×10^4 cfu/cm^2, and colibacillus (*E. coli*) reduced from 228×10^4 cfu/cm^2 leading to bacteria-free adhesion.

Keywords Titanium dioxide, Carrying silver, Dopamine, Silicone, Antibacterial

Polymers are important in tissue engineering, medical devices, and medical carriers[1–3]. Unlike metals and ceramics, polymers can be applied in specific scenarios due to their unique structure and properties[4–6]. Silicone has good aging resistance, mechanical properties, and biological inertia. It also has a wide temperature range and weak inflammatory reactions with human tissues; it is widely used in implanted materials in medicine including urinary catheters, peritoneal dialysis catheters, central venous catheters, and endotracheal catheters[7–18].

Medical devices made from silicone usually make contact with human tissues. In this process, bacteria (such as Staphylococcus aureus, Escherichia coli, and Proteus) easily invade the tissue through various ways causing infection[19–22]. According to the US Centers for Disease Control and Prevention, 15–25% of hospitalized patients require catheter catheterization. Almost all of the patients undergoing long-term catheterization will develop positive urine cultures within a month; 44% are contaminated within two weeks. The patient's risk of infection increases based on the time that the device stays in the body[23]. Therefore, the antibacterial properties of medical silicone material are particularly important.

Nano-titanium dioxide and nanosilver particles are widely used in the field of antibacterial modification and have excellent antibacterial performance[24,25]. However, their distribution in the modification matrix can be decreased by the high specific surface area of nanomaterials, thus leading to a performance decline.

Dopamine can form polydopamine via polymerization and subsequently coat the surface of different matrices. Due to its adhesion, reduction, and biocompatibility, dopamine and its derivatives have been used in different fields. Here, the dispersion and interface binding ability of nanoparticles were improved via a silicone matrix with a multi-step modification.

[1]Changzhou University Huaide College, Jingjiang 214500, China. [2]Changzhou Vocational Institute of Textile and Garment, Changzhou 213000, China. [3]Changzhou University, Changzhou 213000, China. ✉email: 739884923@qq.com

Materials and methods

Materials

Nano-titanium dioxide (TiO_2), dopamine, and 2,5-dimethyl-2,5-di (tert-butylperoxy) hexane, were purchased from Aladdin Bio-Chem Technology Co., Ltd. (Shanghai, China). Silver nitrate, acetone, and trihydroxymethyl-aminomethane, were purchased from China National Pharmaceutical Group Co., Ltd. (Shanghai, China). Silicone was purchased from Xinghuo Organic Silicone Plant (Jiangxi, China). Hydrochloric acid was purchased from Yonghua Chemical Technology Co., Ltd. (Jiangsu, China).

Preparation of silver-carrying nano-TiO_2antimicrobial agents

0.788 g of Trihydroxymethyl aminomethane and 14.7 ml 0.1 mol/L hydrochloric acid was added to the beaker. The deionized water was slowly added the solution and stir at 25 °C. Use a pH meter to detect the pH value of the solution. When the pH value of the buffer is 8.5, stop adding deionized water and seal the resulting solution for low-temperature storage.

Then, 0.5 g of TiO_2 was added to the trihydroxymethylaminomethane-hydrochloric acid mixture. The sample was then sonicated for 30 min. After dispersion, 1.5 g of dopamine was added, and the reaction was stirred for 36 h at room temperature. After the reaction, the products were centrifugally washed three times using deionized water (9000 r/min, 10 min) and subsequently placed in a 60 °C vacuum oven and dried for 24 h to prepare dopamine-coated nano-titanium dioxide (TiO_2-PDA).

TiO_2-PDA particles (1 g) were placed into 100 ml of solution $AgNO_3$ (the concentration is 50 mg/mL); the reaction was shaken for 24 h at room temperature. After the reaction, the resulting products were Centrifugally washed three times with deionized water (9000 r/min, 10 min). They were then placed in a 60 °C vacuum oven and dried for 24 h and ground into powder to prepare dopamine-coated silver-carrying nano-titanium dioxide antibacterial agents, i.e., TiO_2-PDA-Ag particles.

Preparation of antimicrobial-resistant silicone composites

The TiO_2-PDA-Ag particles were mixed with silicone at different proportions via an internal mixer (PPT-3, Putong Instrument, Guangzhou, China) at 25 °C. After mechanical mixing at 30 r/min for 6 min, the composite was then placed into a 1-mm mold and sulfurized using a plate vulcanization machine (XH-406B, Zhengyuan Technology, Dongguan, China) under 175 °C for 9 min. The sample was subsequently vulcanized at 200 °C for 4 h to create an antibacterial silicone test piece.

SEM analysis

SEM (SUPRA55, Carl Zeiss Inc., Germany) evaluated the microscopic morphology of TiO_2-PDA-Ag particles. The antibacterial silicone composite was frozen fracture. The micromorphology of the section was observed after gold sputtering.

TEM Analysis

TEM (JEM-2100, Carl Zeiss Inc., Germany) was used to observe the TiO_2-PDA-Ag particle micromorphology. The sample was prepared at 0.4 mg/ml in anhydrous ethanol. Some solution was dropped on the copper web, and the solvent was evaporated under a vacuum.

XPS analysis

XPS (PHI5000VersaprobeII, Ulvac-Phi, Japan) was used to characterize the elemental composition changes of TiO_2 before and after modification; it used tablets prepared after sample drying. Carbon element was calibrated when using the XPS eqiupment, the binding energy of C–C was 284.8 eV.

XRD analysis

XRD (D/max2500PC, Rigaku, Japan) was used to characterize the crystal structure changes of TiO_2 before and after modification; it used a scanning range of 5° to 80°.The X-RAY source is a Cu target, with $\lambda = 1.54056$ Å.

Antibacterial performance test

Preparation of liquid culture medium and activation and inoculation of bacteria: According to the formula of bacterial liquid culture medium in Table 1, the tryptic liquid culture medium was disinfected three times before

Name	Liquid medium	Solid medium
Beef extract	5 g	5 g
Tryptone	10 g	10 g
NaCl	5 g	5 g
Agar–agar	–	20 g
Purified water	1000 g	1000 g

Table 1. Bacterial adhesion experiment and medium formulation.

inoculation with Bacillus subtilis and Escherichia coli. The sealed sample was incubated for 8 h at 37.5 °C in a 120-rpm shaker.

Preparation of solid medium: Trypsin solid medium was prepared according to the solid medium formula in Table 1 and disinfected three times at 100 °C. Subsequently, 20 ml of solid medium was absorbed by a liquid pipette gun and then cooled, solidified, and UV disinfected for 30 min.

Bacterial adhesion experiment: We next placed the sample in a liquid culture medium, and placed it in a shaker at 37 °C for 8 h. After the shake, the sample was removed, washed slightly with sterile water, put into a test tube containing 10 mL of sterile water, and sonicated for 5 min to obtain a bacterial dispersion. The bacterial dispersion (1 mL) was removed by a pipette gun and placed in 9 mL of sterile water and diluted sequentially to obtain bacterial dispersion with different concentration gradients. After absorbing 0.1 mL of bacterial dispersion and evenly coated on the surface of the solid medium, and incubating in a 37 °C constant temperature incubator for 12 h, the colonies of bacteria in the solid medium at different dilutions were counted.

Calculation of bacterial adhesion on silicone surface: The bacterial adhesion before and after sample modification can be calculated according to formula:

$$N = \sum C/(n_1 + 0.1n_2) \times d$$

where N is the number of sample colonies; ΣC is the total number of plate colonies; n1, n2 are the numbers of plates of the first and second dilutions; and d is the dilution factor.

Mechanical properties test

Use a universal testing machine to measure the tensile properties of the sample according to the standard GB/T 528–2009, with a rate set at 100 mm/min. Measure the tear strength of the sample according to the standard GB/T529-2008, with a rate set at 500 mm/min.

Results

The mechanism of dopamine oxidation autopolymerization and its in situ reduction are shown in Fig. 1[26], and the flowchart of silver-carrying nano-TiO_2 preparation is shown in Fig. 2[27].

Scanning electron microscopy (SEM) observation of the particles

SEM identified similarities and differences between nanoparticles. Figure 3a,b are nano-TiO_2 and TiO_2-PDA-Ag SEM images, respectively. Figure 3c is an EDS image of TiO_2-PDA-Ag. Unmodified nanoparticles are poorly dispersed due to nanoscale effects as shown in Fig. 3a. After polydopamine coating, the TiO_2-PDA-Ag particle morphology is significantly smaller than unmodified nanoparticles, and its dispersion is significantly improved. No obvious agglomeration appears in Fig. 3b, which suggests that the polydopamine coating on the surface of nano-titanium dioxide plays a key role in improving the agglomeration behavior of nanoparticles. This proves that the polydopamine coating can hinder the attraction between nanoparticles and enhance the nanoparticle dispersion. EDS energy spectrum characterization showed many silver points (pink signals) in Fig. 3c, which confirm that silver is present on nano-TiO_2 after dopamine modification.

Transmission electron microscopy (TEM) observation of the particles

TEM was used to study the nano-TiO_2 during modification including microstructural changes. Figure 4a shows unmodified TiO_2, and Fig. 4b shows TiO_2-PDA-Ag TEM images. The surface of nano-TiO_2 before modification is rough, the edge is uneven, and the agglomeration phenomenon is serious, thus it is difficult to separate via ultrasound. Post-modification nanoparticles are shown in Fig. 4b: The nanoparticle aggregation was improved. Black dots are found on the surface of the particles. The characterization results above suggest that these points are silver particles. Silver particles are embedded in the polydopamine coating on the surface of the modified nano-titanium dioxide. That is, TiO_2-PDA-Ag forms a relatively stable structural state with titanium dioxide in the inner layer, polydopamine coated in the outer layer, and the silver particles distributed relatively evenly in the polydopamine-coated layer.

X-ray photoelectron spectroscopy (XPS) analysis of particles

XPS was used to explore the elemental composition of nanoparticles during modification. Figure 5a,b are the X-ray diffraction spectra of nano-TiO_2 and TiO_2-PDA-Ag, respectively. Figure 5c shows the 3D high-resolution profile of silver. Table 2 shows the elemental composition before and after modification of TiO_2. TiO_2 has Ti and O peaks (Fig. 5a). Versus Fig. 5b, the characteristic peak of N 1S appears at 400 eV, and the characteristic peak of C is significantly enhanced because polydopamine is coated on the surface of nano-titanium dioxide. A strong Ag peak appears in Fig. 5b, which proves the existence of Ag after modification. Table 2 shows that the elemental composition changes after dopamine is coated with nano-titanium dioxide and silver carrying modifications. The amount of C and N in TiO_2-PDA-Ag increases, and Ag elements appear due to the inclusion of many C and N elements in the polydopamine structure and the silver on the surface. Figure 5c shows silver and silver oxide peaks at 373.7 eV and 367.7 eV in the spectrum diagram. After Ag particles are reduced to simple substances, they are easier to be oxidized by air, and some of them form silver oxides.

X-ray diffraction (XRD) analysis of particles

XRD was used to explore the crystal structure of nanoparticles during modification. Figure 6a,b are the XRD spectra of TiO_2 and TiO_2-PDA-Ag, respectively. Dopamine modification and the crystal structure of nanoparticles carrying silver were determined by X-ray diffraction instrument. Figure 6a shows peaks at $2\theta = 25.3°$, which

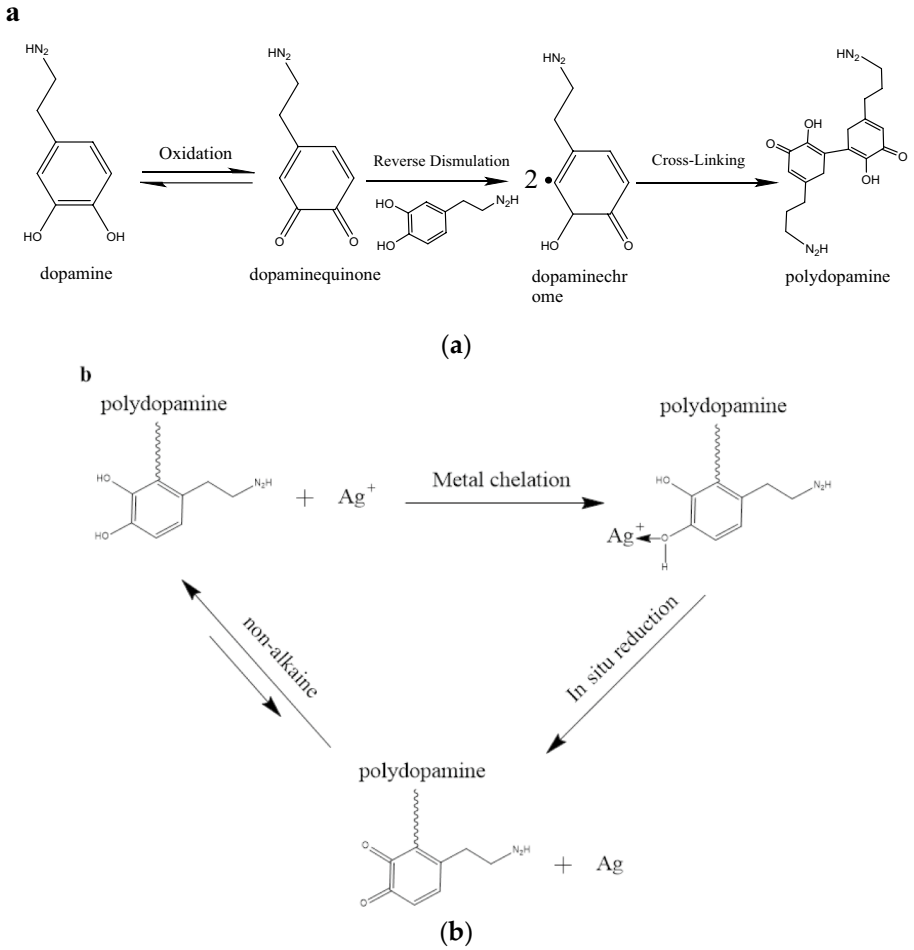

Figure 1. (**a**) Mechanism of dopamine autolpolymerization; (**b**) mechanism of in situ reduction of Ag with dopamine.

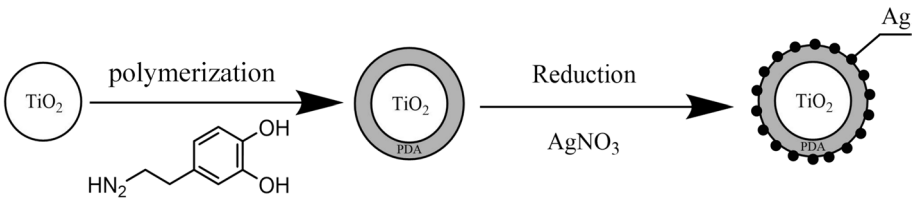

Figure 2. Preparation flowchart of silver-carrying nano-titanium dioxide.

is the anatase characteristic peak of titanium dioxide. Figure 6b shows that the characteristic crystallization peak of silver appeared in the TiO_2-PDA-Ag structure with distribution at $2\theta = 38.1°$, 44.3°, and 64.4° corresponding to (1 1 1), (2 0 0), and (2 2 0), respectively. This proves that the modified polydopamine on the surface of nano-titanium dioxide successfully reduces the silver. Crystalline diffraction peaks of nano-TiO_2 also exist. These data indicate that polydopamine is only coated on the surface of nano-TiO_2, and the silver particles on the surface did not enter the nano-TiO_2 lattice (this would not change the TiO_2 structure).

Microstructure of silicone composites

To study the dispersibility of TiO_2-PDA-Ag particles in silicone, pure silicone and composite materials supplemented with antibacterial agents were frozen with liquid nitrogen, and their sections were observed using scanning electron microscopy. Figure 7a,b are SEM images magnified 20,000 times; Fig. 7a is the section SEM of silicone without antibacterial agents, and Fig. 7b is an SEM image of silicone after adding antibacterial agents. Figure 7a shows that the continuous phase is very uniform. White particles are evenly distributed in the modified silicone section in Fig. 7b, and the particle diameter is still on the nanoscale. The results show that TiO_2-PDA-Ag antibacterial particles have good dispersibility in silicone.

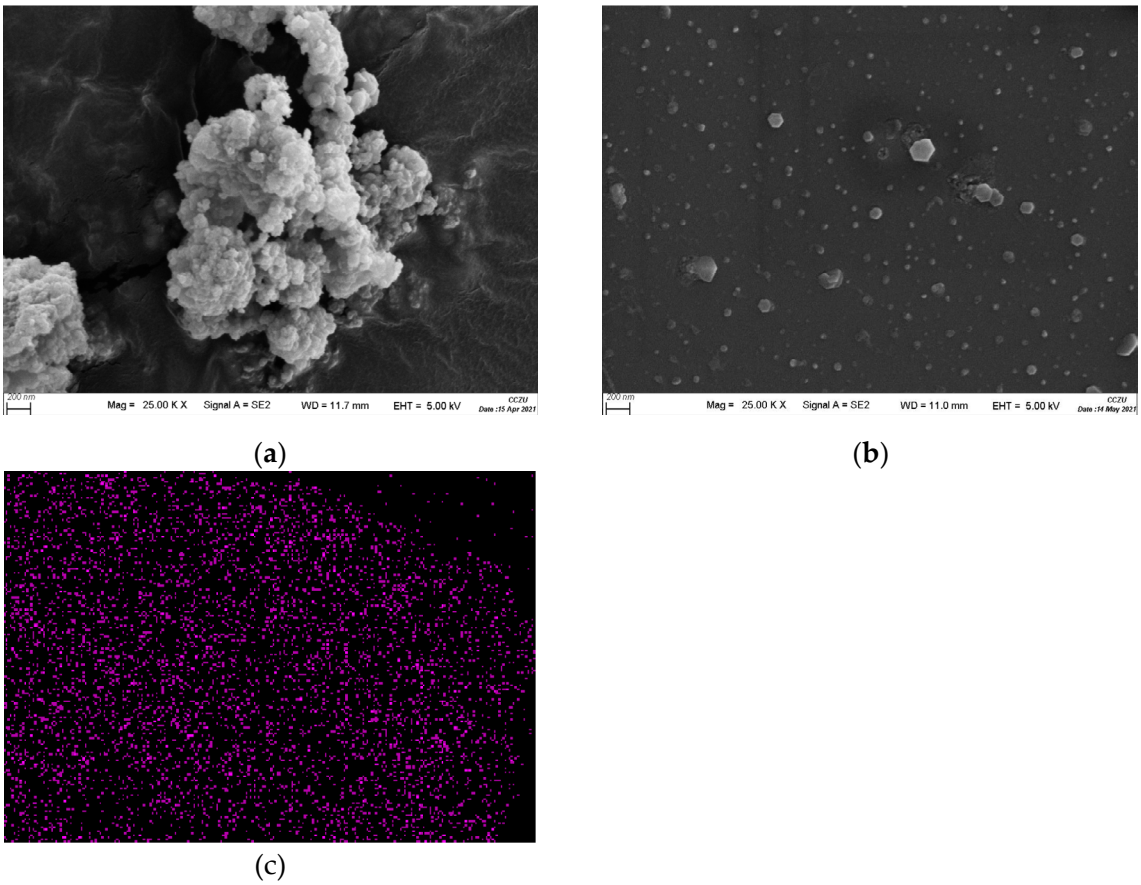

Figure 3. SEM and images of particles: (**a**) TiO_2 ; (**b**) TiO_2-PDA-Ag ; (**c**) EDS (Ag).

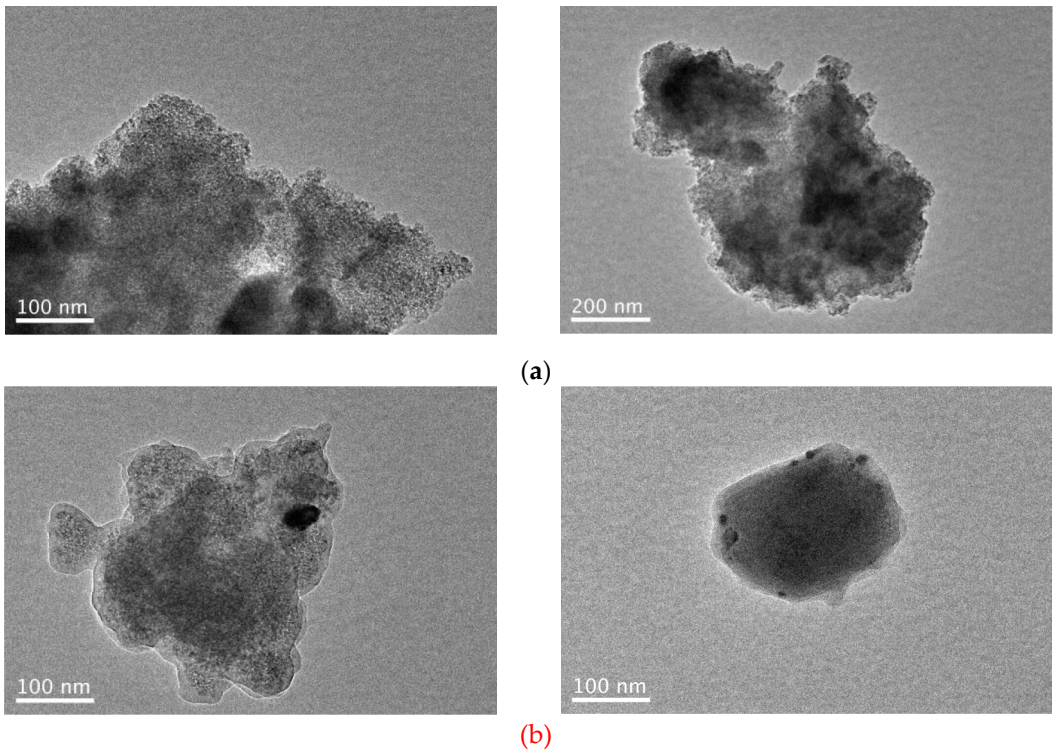

Figure 4. High-resolution transmission electron microscope images of particles: (**a**) TiO_2 ; (**b**) TiO_2-PDA-Ag.

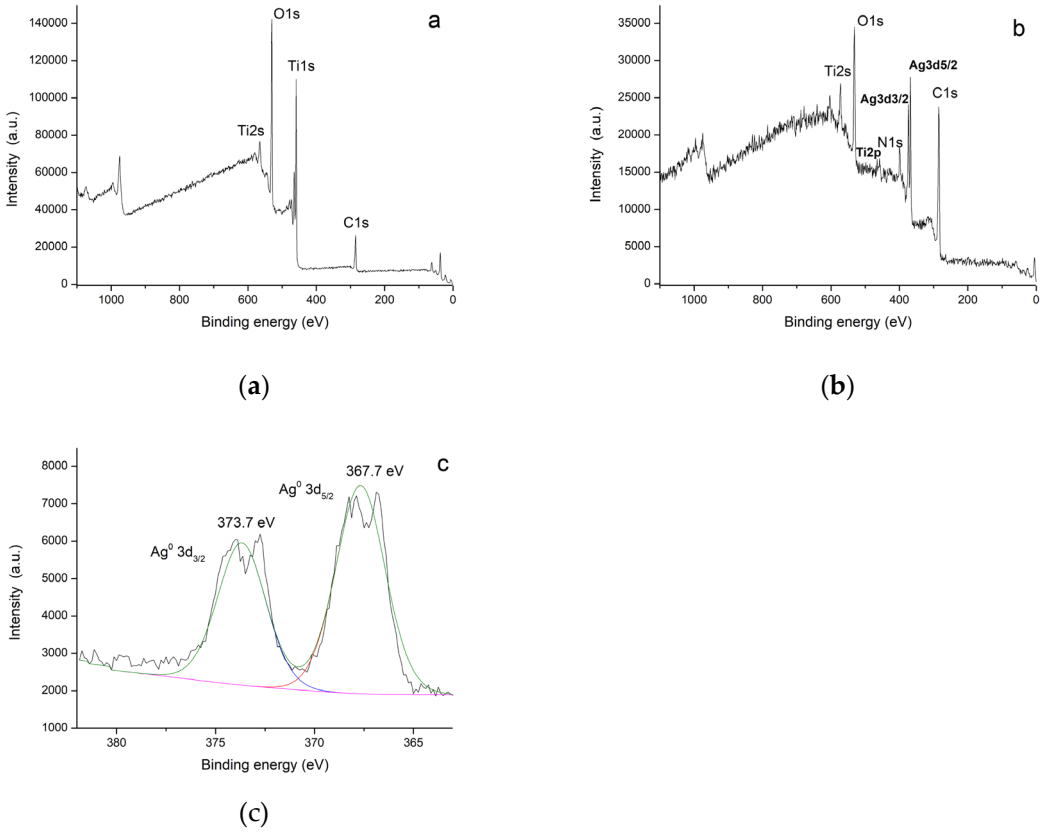

Figure 5. X-ray diffraction spectrum: (**a**) TiO_2 ; (**b**) TiO_2-PDA-Ag; (**c**) 3D high-resolution spectrogram of silver.

Sample	C	N	O	Ti	Ag
TiO_2	29. 73%	0. 29%	50. 90%	20. 17%	-
TiO_2-PDA-Ag	54. 55%	6. 53%	22. 11%	12. 35%	4. 46%

Table 2. Elemental composition before and after modification of TiO_2.

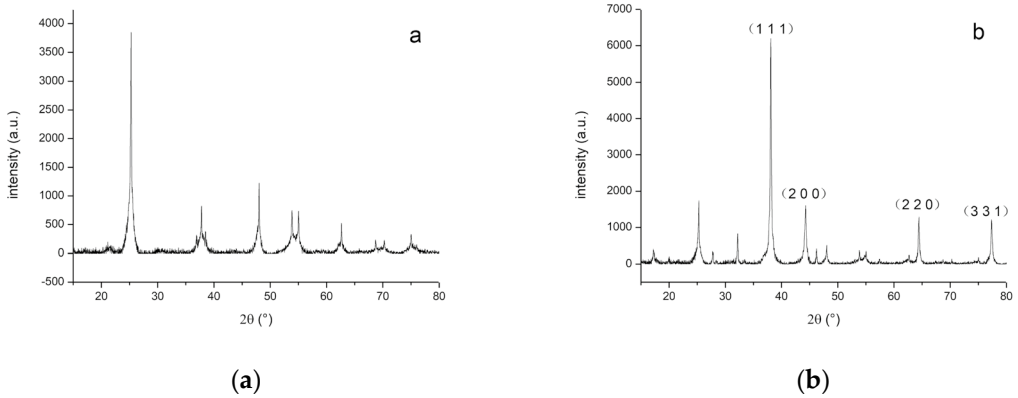

Figure 6. XRD spectra: (**a**) TiO_2 ; (**b**) TiO_2-PDA-Ag.

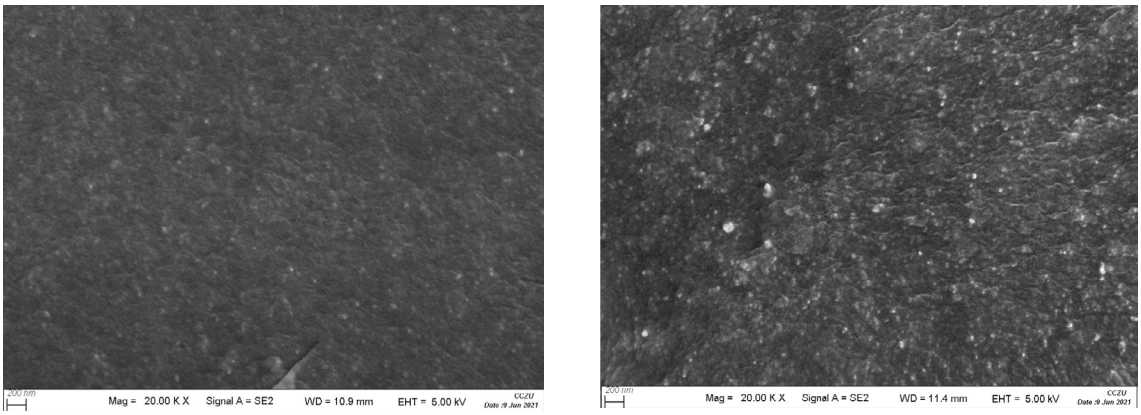

(**a**) (**b**)

Figure 7. Scanning electron micrograph of cross-section: (**a**) silicone; (**b**) composites.

Antibacterial properties of silicone composites

The antibacterial properties of silicone composites with different contents of antibacterial agents were evaluated by the plate counting method as shown in Fig. 8. The addition of different proportions of nano-TiO_2-PDA-Ag particles modified *E. coli* and *B. subtilis* adhesion. The adhesion of *E. coli* and Bacillus subtilis on the pure silicone surface is very high . There was an increase in the amount of nano-antibacterial agents, and the amount of bacterial adhesion on the surface gradually decreased. The results show that the corresponding *B. subtilis* adhesion changed from 246×10^4 cfu/cm^2 to 2×10^4 cfu/cm^2 (antibacterial activity of 99.2%). For *E. coli*, there was 100% antibacterial activity. This is because nanoparticles enhances the antibacterial activity of the silicone composites. The silver ions have a positive charge, and bacteria are negative. This attraction leads to protein solidification, which destroys the activity of cell synthases as well as proteases. In turn, there is a loss of cell proliferation and thus cell death[28]. The cell wall of Gram-positive bacteria is generally thicker than that of Gram-negative bacteria. B. subtilis was the kind of Gram-posetive and E.coli was the kind of Gram-negative. The antibacterial properties of silver ions are mainly manifested in their ability to destroy the cell wall. So the bactericidal ability of silver carrying nanocomposites against B. subtilis is weaker than that of E.coli.

Mechanical properties of antibacterial silicone rubber composite materials

In Fig. 9, it can be observed that as the amount of antibacterial agent added increases, the tensile strength, elongation at break, and tear strength of the composite material show a decreasing trend but are not significant. This is because the addition of antibacterial agents has a certain degree of damage to the structure of silicone rubber itself; As the amount of antibacterial agent added increases, its disrupte the perfect three-dimensional network structure of silicone rubber, ultimately leading to stress concentration points inside the body structure of silicone rubber composite materials, resulting in a decrease in the overall mechanical properties of the composite materials.

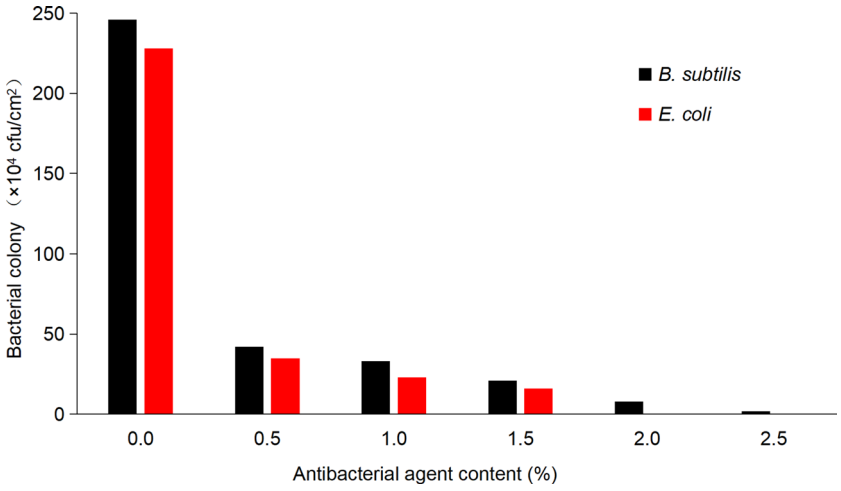

Figure 8. Antibacterial properties of silicone after adding different proportions of antibacterial agents.

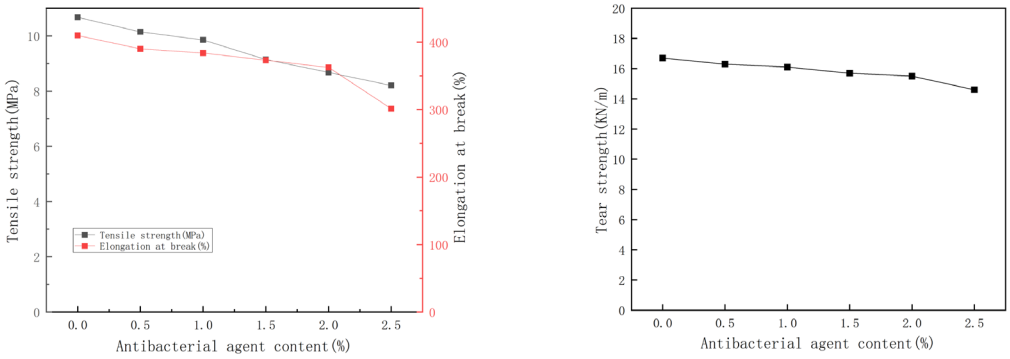

(a) (b)

Figure 9. Mechanical properties of antibacterial silicone rubber composite materials. (**a**) tensile strength and elongation at break, (**b**) tear strength.

Conclusions

TiO_2-PDA-Ag form a relatively stable core–shell structure. The inner layer is titanium dioxide, and the outer layer is coated with polydopamine. The silver particles are evenly distributed in the polydopamine coating layer. There were relatively clear characteristic peaks in XPS and XRD after centrifugal cleaning, thus indicating nano-TiO_2 had PDA and Ag particles in the outer layer. The system is relatively stable. TiO_2-PDA-Ag antibacterial agents have good dispersion in silicone composite materials as well as excellent antibacterial performance. When the amount of antibacterial agent is 2.5%, the antibacterial activity of the composite material is 99.2% for *B. subtilis* and 100% for *E. coli*.

Data availability

Data is available on request from Dongdong Hao (haodongdong@ smail.cczu.edu.cn).

Received: 12 June 2024; Accepted: 8 August 2024
Published online: 14 August 2024

References

1. Haider, A., Haider, S. & Kang, I. K. A comprehensive review summarizing the effect of electrospinning parameters and potential applications of nanofibers in biomedical and biotechnology. *Arab. J. Chem.* **11**, 1165–1188 (2018).
2. Feng, P. *et al.* Characterizations and interracial reinforcement mechanisms of muhicomponent biopolymer based scaffold. *Mater. Sci. Eng. C* **100**, 809–825 (2019).
3. Wendels, S. & Avérous, L. Biobased polyurethanes for biomedical applications. *Bioact. Mater.* **6**, 1083–1106 (2021).
4. Mei, J. *et al.* Biocompatibility of biomedical polymer materials and its surface modification technologies. *Materials Review* **28**, 139–142 (2014).
5. Holzapfel, B. M. *et al.* How smart do biomaterials need to be? A translational science and clinical point of view. *Adv. Drug Deliv. Rev.* **65**, 581–603 (2013).
6. Manavitehrani, I. *et al.* Biomedical applications of biodegradable polyesters. *Polymers* **8**, 20 (2016).
7. Xu, R., Luo, G. & Xia, H. Novel bilayer wound dressing composed of silicone with particular micropores enhanced wound re-epithelialization and contraction. *Biomaterials* **40**, 1–11 (2015).
8. Feng, P. *et al.* A mu/timaterial scaffold with tunable properties: Toward bone tissue repair. *Adv. Sci.* **5**, 1700817 (2018).
9. Zhu, Z., Wang, Z., Li, S. & Yuan, X. Antimicrobial strategies for urinary catheters. *J. Biomed. Mater. Res. Part A* **107**, 445–467 (2019).
10. Shuai, C. *et al.* A graphene oxide–Ag co–dispersing nanosystem: Dual synergistic effects on antibacterial activities and mechanical properties of polymer scaffolds. *Chem. Eng. J.* **347**, 322–333 (2018).
11. Gomes, R. N. *et al.* Antimicrobial graphene nanoplatelets coatings for silicone catheters. *Carbon* **139**, 635–647 (2018).
12. Grigoryan, B. *et al.* Muhivascular networks and functional intravascular topologies within biocompatible hydrogels. *Science* **364**, 458–464 (2019).
13. Li, Y. T. *et al.* Processing, thermal conductivity and flame retardant properties of silicone rubber filled with different geometries of thermally conductive fillers: A comparative study. *Composites Part B* **238**, 109907 (2022).
14. Shi, G. *et al.* Highly sensitive, wearable, durable strain sensors and stretchable conductors using graphene/silicon rubber composites. *Adv. Funct. Mater.* **26**, 7614–7625 (2016).
15. Bouty, A. *et al.* Nanofiller structure and reinforcement in model silica/rubber composites: A quantitative correlation driven by interfacial agents. *Macromolecules* **47**, 5365–5378 (2014).
16. Miranda, I. *et al.* Properties and applications of PDMS for biomedical engineering: A review. *J. Funct. Biomater* **13**, 2 (2022).
17. Kim, S. J., Lee, D. S., Kim, I. G., Sohn, D. W. & Kim, S. W Evaluation of the biocompatibility of a coating material for an implantable bladder volume sensor. *Kaohsiung J. Med. Sci.* **28**, 123–129 (2012).
18. Zare, M., Ghomi, E. R., Venkatraman, P. D. & Ramakrishna, S. Silicone-based biomaterials for biomedical applications: Antimicrobial strategies and 3d printing technologies. *J. Appl. Polym. Sci.* **138**, 50969 (2021).
19. Magennis, E. P., Hook, A. L., Williams, P. & Alexander, M. R. Making silicone highly resistant to bacterial attachment using thiol-ene grafting. *ACS Appl. Mater. Interfaces* **8**, 30780–30787 (2016).
20. Liu, Y. *et al.* Antibacterial graphene oxide coatings on polymer substrate. *Applied Surface Science* **436**, 624–630 (2018).

21. Xu, R. *et al.* Novel bilayer wound dressing composed of silicone with particular micropores enhanced wound re-epithelialization and contraction. *Biomaterials* **40**, 1–11 (2015).
22. Perrin, K. *et al.* Catheter-associated urinary tract infection (CAUTI) in the NeuroICU: Identification of risk factors and time-to-cauti using a case–control design. *Neurocrit. Care* **34**, 271–278 (2021).
23. Saint, S. & Chenoweth, C. E. Biofilms and catheter-associated urinary tract infections. *Infect. Dis. Clin.* **17**, 411–432 (2003).
24. Rezazadeh, N. & Kianvash, A. Preparation, characterization, and antibacterial activity of chitosan/silicone rubber filled zeolite, silver, and copper nanocomposites against Pseudomonas aeruginosa and methicillin-resistant Staphylococcus aureus. *J. Appl. Polym. Sci.* **138**, 50552 (2021).
25. Yu, Y., Yang, Z., Ren, S., Gao, Y. & Zheng, L. Multifunctional hydrogel based on ionic liquid with antibacterial performance. *J. Mol. Liq.* **299**, 112185 (2020).
26. Ball, V., Nguyen, I., Haupt, M., Oehr, C. & Ruch, D. The reduction of Ag+ in metallic silver on pseudomelanin films allows for antibacterial activity but does not imply unpaired electrons. *J. Colloid Interface Sci.* **364**, 359–365 (2011).
27. Qureshi, D. A. *et al.* Why mussel byssal plaques are tiny yet strong in attachment. *Matter* **5**, 710–724 (2022).
28. Zhu, S. *et al.* Dual functional polylactide–hydroxyapatite nanocomposites for bone regeneration with nano-silver being loaded via reductive polydopamine. *RSC Adv.* **6**, 91349–91360 (2016).

Acknowledgements

With many thanks to my supervisor, Yonghong Ding ,for his guidance during this research.

Author contributions

D.H. and Y.D. designed the experiments; Y.Z. and D.H. performed the experiments; D.H. analyzed the data; Y.Z. wrote the draft; D.H., Y.D. and Q.Y. revised the paper; D.H. provided funding acquisition. All authors have read and agreed to the published version of the manuscript.

Funding

This research was funded by Jiangsu Qing Lan Project(No. SCZ2363220001).

Competing interests

The authors declare no competing interests.

Additional information

Correspondence and requests for materials should be addressed to Y.Z.

Reprints and permissions information is available at www.nature.com/reprints.

Publisher's note Springer Nature remains neutral with regard to jurisdictional claims in published maps and institutional affiliations.